used instead of pyridine[1] which others have implicated in PEG decomposition.[30] The pale yellow $SOCl_2$/toluene solution is slowly added over ca. 20 min to the stirred MePEG/toluene solution, and after a 2-h reflux the crude MePEG-Cl (**2**) solution is reduced to a viscous melt at reduced pressure in a rotary evaporator. Taking up the brownish polymer in 150 mL of dried (K_2CO_3) CH_2Cl_2, the solution was filtered, degassed with Ar, treated with 50 g of activated alumina in a 500-mL flask for 30 min to remove traces of $SOCl_2$, filtered, and reduced to 30 mL, 150 mL of ether was added, and the solution was cooled in the freezer for 2 h after which 15.1 g (yield 79%) of off-white powder MePEG-Cl (**2**) was collected: IR (KBr pellet) 1110 cm^{-1} (CH_2OCH_2), 669 cm^{-1} (CCl) and no detectable OH absorption at 3300–3500 cm^{-1}.

MePEG-N_3[$CH_3O(CH_2CH_2O)_nCH_2CH_2N_3$], 3. NaN_3 (3.3 g, 51 mmol) was added with stirring to 12 g (6.3 mmol) of MePEG-Cl (**2**) in 100 mL of DMF (dried over 4 Å molecular sieves and freshly vacuum distilled[31]) heated under Ar to 120 °C (oil bath) in a flask equipped with reflux condenser. After stirring at 120 °C for 4 h, the solution was cooled to room temperature and filtered, the DMF was removed under reduced pressure in a rotary evaporator, the viscous polymer melt was taken up in 50 mL of CH_2Cl_2, and filtered, 150 mL of ether was added, and the solution was cooled in the freezer for 2 h. The collected precipitate was reprecipitated once further and 11 g (92% yield) of MePEG-N_3 (**3**) was collected as an off-white power: IR (KBr pellet) 2108 cm^{-1} (N_3^-), 1110 cm^{-1} (CH_2OCH_2), and no absorption for Cl at 669 cm^{-1}.

MePEG-$NH_3^+Cl^-$, [$CH_3O(CH_2CH_2O)_nCH_2CH_2NH_3^+Cl^-$], 4. MePEG-$N_3$ (**3**) (10.0 g, 5.3 mmol), 60 mL of absolute EtOH, and 20 mL of CH_2Cl_2 purged with Ar in a Parr bottle, to which 1.5 g of 5% Pd(C) was added, hydrogenated overnight at 50 psi H_2. The product solution was filtered through Celite and then through a 0.45-μm syringe filter (Gelman Sciences) to remove residual catalyst, and the solvent was pumped off. The crude product was taken up in 20 mL of CH_2Cl_2 and 100 mL of ether and was chilled in the freezer for 2 h; the precipitate was collected and reprecipitated to yield 7.5 g (75%) of a white powder: IR (KBr pellet) 3300 cm^{-1} (NH_3^+), 1110 cm^{-1} (CH_2OCH_2), and no absorption for N_3 at 2108 cm^{-1}.

Fc-MePEG, [$CH_3O(CH_2CH_2O)_nCH_2CH_2NH(CO)CpFeCp$], 5. MePEG-$NH_3^+Cl^-$ (4) (0.95 g, 0.5 mmol), 0.12 g (0.5 mmol) of ferrocene carboxylic acid, 0.07 g (0.5 mmol) of 1-hydroxybenzotriazole, 0.12 g (0.6 mmol) of dicyclohexylcarbodiimide, 0.14 mL (1.0 mmol) of triethylamine, and 50 mL of CH_2Cl_2 in a sealed flask were stirred in the dark for 5 days and filtered. Ether was added after standing in the freezer for 2 h, and 0.84 g of crude Fc-MePEG (**5**) was collected. This product, dissolved in 2.0 mL of water was centrifuged to remove an insoluble white material and subjected to chromatography on a 1.7 × 20 cm phenylsepharose (Pharmaceia, CL-4B) column, eluting with 0.5 M $(NH_4)_2SO_4$. (This gel column was stored in 20% EtOH, after washing, in order, with 100 mL each of 0.5 M $(NH_4)_2SO_4$, distilled H_2O, and 20% EtOH and was prepared for use by the reverse of this procedure.) The single orange-colored band was collected, extracted with CH_2Cl_2 (3 × 10 mL), precipitated with ether, and dried in a vacuum desiccator at room temperature for 24 h to yield 0.50 g (53% yield; 29% yield overall MePEG) of pale orange powder Fc-MePEG (**5**): IR 1649 cm^{-1} (C–O, amide), 1110 cm^{-1} (CH_2OCH_2), no absorption for NH_2 at 3324 cm^{-1}; ^{13}C NMR (100.6 MHz, $CDCl_3$) 38.4, 58.2, 67.6, 69.7, 75.9, 76.2, 76.4 ppm. Elemental anal. Calcd for [$CH_3O(CH_2CH_2O)_{52.4}CH_2CH_2NH(CO)$-$CpFeCp$] ($C_{118.8}H_{226.6}Fe_1N_1$): C, 55.09; H, 8.78, N, 0.54; Fe, 2.16. Found: C, 55.10; H, 8.56; N, 0.63; Fe, 1.86.

Acknowledgment. Y.L.M. acknowledges with gratitude a NATO Fellowship. The research was supported in part by grants from the Department of Energy (DE-FG05-87ER13675) and the National Science Foundation.

(28) Nicholson, R. S. *Anal. Chem.* **1965**, *37*, 1351.
(29) (a) Bond, A. M.; Henderson, T. L. E.; Mann, D. R.; Mann, T. F.; Thormann, W.; Zoski, C. G. *Anal. Chem.* **1988**, *60*, 1878. (b) Kadish, K. M.; Ding, J. Q.; Malinski, T. *Anal. Chem.* **1984**, *56*, 1741.
(30) (a) Harris, J. M.; Yalpani, M.; Van Alstine, J. M.; Struck, E. C.; Case, M. G.; Paley, M. S.; Brooks, D. E. *J. Polym. Sci., Polym. Ed.* **1984**, *22*, 341. (b) Harris, J. M.; Hundley, N. H.; Shannon, T. G.; Struck, E. C. *J. Org. Chem.* **1982**, *47*, 4789.
(31) Perrin, D. D.; Armagero, W. L. F.; Perrin, D. R. *Purification of Laboratory Chemicals*, 2nd ed.; Pergamon Press: New York, 1980.

The Effect of Pressure on the Surface Plasmon Absorption Spectra of Colloidal Gold and Silver Particles

Jeffery L. Coffer, John R. Shapley,* and Harry G. Drickamer*

Contribution from the School of Chemical Sciences, Department of Physics, and Materials Research Laboratory, University of Illinois, Urbana—Champaign, Urbana, Illinois 61801.
Received December 19, 1989

Abstract: The first measurements of the effect of pressure on the peak position (ω_{sp}) and line width (fwhm) of the surface plasmon absorption in several Au and Ag hydrosols have been recorded up to 10 kbar. Red shifts of the plasmon peak with increasing pressure are observed for relatively large metal particles prepared by the citrate procedure (Au, $\bar{d}$ = 265 Å; Ag, $\bar{d}$ = 230 Å). The shift for silver is over twice that of gold (−420 cm^{-1} vs −200 cm^{-1}). These red shifts are interpreted in terms of pressure-induced volume changes within the context of a free-electron model. In contrast, particles prepared by the Faraday method (Au, $\bar{d}$ = 54 Å; Ag, $\bar{d}$ = 60 Å) show initial blue shifts with pressure, with the magnitude again larger for silver. Upon aging (as well as upon heating in the case of Au), the Au and Ag Faraday sols exhibit an increase in their average particle size and degree of aggregation. Correspondingly, the pressure response of their plasmon absorption approaches that of the citrate sols.

Interest in the physicochemical properties of colloidal metal particles has been ongoing since the time of Faraday, who demonstrated that colloidal gold particles can be formed in a facile manner by reduction of an aqueous gold salt solution with white phosphorus.[1] Current efforts focus on a number of different areas and applications. One is the area of catalysis, where workers have investigated the reactivity of colloidal metal particles on oxide supports[2] as well as implicated metal colloids as the active species in a number of reactions previously thought to be homogeneously catalyzed.[3] Additional studies have also examined colloidal metal particles for applications as biological stains[4] and ferrofluids.[5] On a fundamental level, the issue of "quantum size effects" is an

(1) Faraday, M. *Philos. Trans.* **1857**, *147*, 145.
(2) (a) Bradley, J. S.; Leonowicz, M. E.; Witzke, H. *J. Mol. Catal.* **1987**, *41*, 59. (b) Thomas, J. M. *Pure Appl. Chem.* **1988**, *60*, 1517.
(3) (a) Lewis, L. N.; Lewis, N. *J. Am. Chem. Soc.* **1986**, *108*, 7228. (b) Lewis, L. N.; Lewis, N. *J. Am. Chem. Soc.* **1986**, *108*, 743. (c) Picard, J. P.; Dunogues, J.; Elyussfi, A. *Synth. Commun.* **1984**, *14*, 95. (d) Freeman, F.; Kappos, J. C. *J. Am. Chem. Soc.* **1985**, *107*, 6628. (e) Maier, W. F.; Chettle, S. J.; Rai, R. S.; Thomas, G. *J. Am. Chem. Soc.* **1986**, *108*, 2608. (f) Burk, P. L.; Pruett, R. L.; Campo, K. S. *J. Mol. Catal.* **1985**, *33*, 1.
(4) (a) Faulk, W.; Taylor, G. *Immunochem.* **1971**, *8*, 1081. (b) Roth, J.; Bendayan, M.; Orci, L. *J. Histochem. Cytochem.* **1980**, *28*, 55.
(5) Charles, S. C.; Popplewell, J. In *Ferromagnetic Materials*; Wohlharth, E. P., Ed.; North Holland: Amsterdam, 1980; Vol. 2.

0002-7863/90/1512-3736$02.50/0

actively debated topic, with a number of experimental approaches currently being utilized.[6]

A characteristic feature of gold and silver colloids is the discrete band that can be observed in the visible electronic spectrum of these particles, the surface plasmon resonance. For the surface plasmon, i.e., a quantized plasma oscillation at the surface, the experimental features most thoroughly studied are the full width at half maximum (fwhm), and to a lesser extent, the peak location at maximum intensity (ω_{sp}).[7] For metal particles suspended in a glass or in an inert gas at cryogenic temperatures, previous studies suggest an inverse relationship between average particle size and the line width of the surface plasmon peak, with the magnitude of the correlation highly dependent on the nature of the embedding medium.[8] Such observations have been interpreted, with some success, in terms of both classical[9] and quantum mechanical[7c,10] models. Studies of the surface plasmon peak maximum, on the other hand, have failed thus far to establish any firm correlation between the average diameter of the metal particle and peak maximum location.[6a,10b] This is in contrast to the correlation between average particle size and location of the absorption edge for II–VI colloidal semiconductor megaclusters.[11] For colloidal metal particles, several reports have noted slight shifts to higher energy with decreasing particle size.[7b-d] In contrast, a report by Smithard asserts that the plasmon peak location of silver particles in glass shifts slightly red with decreasing particle diameter.[7e] A number of theoretical studies have been undertaken; methods of employing a quantum mechnical "particle-in-a-box" formalism with discrete energy levels predict "blue shifts" with decreasing particle size,[7c,10b,12] while hydrodynamical theories predict the opposite trend.[13]

The application of high pressure has been shown to provide unique information with regard to the electronic structure (i.e. "pressure tuning") of a variety of materials in condensed phases.[14] Thus we decided to probe the effects of high pressure on the surface plasmon resonance of colloidal metal particles. We report here the first measurements of the effect of applied pressure on the surface plasmon resonance of gold and silver colloidal hydrosols. Between silver and gold, distinct differences are observed in the pressure-induced peak shifts for particles prepared by two different methods (citrate and Faraday). The shifts are interpreted in terms of a free-electron gas model for the case of the citrate-derived colloids. We also note in this work the sensitivity of pressure-induced peak shifts to differences in particle size, suggesting the onset of a "quantum size effect" for the smallest particles examined. To our knowledge, the only previous account involving high-pressure spectroscopic investigations of metal colloids was a recent report analyzing the pressure effects on selected vibrations observed for pyridine-adsorbed gold sols.[15]

Table I. Spectroscopic Properties of the Gold Colloids

colloid (size)	E_{max}, $\times 10^3$ cm^{-1}	fwhm, cm^{-1}	E_{max} behavior (in 10 kbar), cm^{-1}
Au citrate (265 Å)	19.14	3500	−200
Au Faraday (54 Å)	19.28	4100	−80[a]
Au Faraday (85 Å) aged 2 months	19.27	3575	−130
Au Faraday (108 Å) aged 4 months	20.00 16.50	3900 5700	−205 −165
Au Faraday (128 Å) heated at 75 °C	19.07	4100	−160

[a] The surface plasmon absorption of this sol initially shifts +20 cm^{-1} in 4 kbar.

Table II. Spectroscopic Properties of Silver Colloids

colloid (size)	E_{max}, $\times 10^3$ cm^{-1}	fwhm, cm^{-1}	E_{max} behavior (in 10 kbar), cm^{-1}
Ag citrate (230 Å)	23.60	5300	−420
Ag Faraday (60 Å)	24.70	4885	−270[a]
Ag Faraday (75 Å) aged 2 months	24.54	5130	−190
Ag Faraday (111 Å) aged 4 months	24.76	5100	−245

[a] The surface plasmon absorption of this sol initially shifts +200 cm^{-1} in 4 kbar.

Experimental Section

Two well-known procedures for metal colloid preparation were chosen: the Faraday method, as modified by Wilenzick et al.,[16] and the citrate reduction procedure of Turkevich, Stevenson, and Hillier.[17] Each method was applied to prepare colloidal particles of either gold or silver, with $HAuCl_4$ (Aldrich) or $AgNO_3$ (Alfa) as metal sources, respectively. Representation of the distribution of particle sizes obtained in terms of log–probability plots (Supplementary Material) reveals that for the citrate and Faraday sols log normal distributions are obeyed, with median particle sizes of 54 and 60 Å obtained for the Au and Ag Faraday sols, respectively, and corresponding values of 265 and 230 Å obtained for the Au and Ag citrate sols. From these log–probability plots, geometric deviations of $\sigma = 1.56$ (Au) and 1.80 (Ag) were obtained for the Faraday sols, with values of 1.35 (Au) and 1.21 (Ag) obtained for the citrate sols. These values of σ are within the range observed previously for metal particles prepared by several different routes.[18] Each sol of identical metal concentration was prepared fresh prior to the corresponding high-pressure spectroscopic studies, with the exception of the aging studies for which solutions were stored in stoppered flasks in the absence of light at room temperature. To examine the effect of heating on the metal particles, a gold Faraday sol was heated at 70–75 °C for 2 h in air.

Particle size determinations of the colloidal metal particles were carried out with either the Philips EM-400 or EM-420 instruments at the Center for Microanalysis of Materials at the University of Illinois. Samples were prepared by placing submicroliter amounts of colloid on a carbon-coated copper grid prior to examination. Confirmation of the identity of the colloidal particles as gold or silver was confirmed by energy-dispersive X-ray analysis (EDAX) of the samples.

For the high-pressure experiments, a 1-mL sample of the colloid was placed in an inner steel cylindrical cell employing sapphire windows as pistons. This cell was placed in a high-pressure bomb,[19] which was then filled with isobutyl alcohol as a pressurizing fluid. The light source used was an Oriel tungsten halogen lamp, with the light dispersed by a Kratos 1/4m monochromator with a 450 blaze grating. Light in the visible region was detected by an EMI 9558 photomultiplier tube along with an Ortec photon counting system. The resulting spectra were fit with a single Gaussian band by means of the computer program SKEW with use of a nonlinear least-squares algorithm. The values obtained for the peak heights, locations, and widths were those that minimized the variance, which for all spectra recorded was on the order of 10^{-4} or less. A tabular listing of variance values is given in the Supplementary Material. All

(6) (a) Halperin, W. *Rev. Mod. Phys.* **1986**, *58*, 533. (b) Kreibig, U.; Genzel, L. *Surf. Sci.* **1985**, *156*, 678. (c) Ozin, G.; Mitchell, S. *Angew. Chem., Int. Ed. Engl.* **1983**, *22*, 674.

(7) (a) Doremus, R. *J. Chem. Phys.* **1964**, *40*, 2389. (b) Doremus, R. *J. Chem. Phys.* **1965**, *42*, 414. (c) Kreibig, U.; Von Fragstein, C. *Z. Phys.* **1969**, *224*, 307. (d) Kreibig, U. *J. Phys. F* **1974**, *4*, 999. (e) Genzel, L.; Martin, T.; Kreibig, U. *Z. Phys. B* **1975**, *21*, 339. (f) Smithard, M. A. *Solid State Commun.* **1974**, *14*, 407. (g) Kreibig, U. *J. Phys.* **1977**, *38*, C2-97.

(8) Charle, K.; Frank, F.; Schulze, W. *Ber. Bunsenges. Phys. Chem.* **1984**, *88*, 350.

(9) Mie, G. *Ann. Phys.* **1908**, *25*, 377.

(10) (a) Wood, D.; Ashcroft, N. W. *Phys. Rev. B* **1982**, *25*, 6255. (b) Cini, M. *J. Opt. Soc. Am.* **1981**, *71*, 389. (c) Cini, M.; Ascarelli, P. *J. Phys. F* **1974**, *4*, 1998. (d) Ruppin, R.; Yatom, H. *Phys. Status Soldi (b)* **1976**, *74*, 647. (e) Kraus, W.; Schatz, G. *J. Chem. Phys.* **1983**, *79*, 6130.

(11) (a) Spanhel, L.; Haase, M.; Weller, H.; Henglein, A. *J. Am. Chem. Soc.* **1987**, *109*, 5649. (b) Weller, H.; Schmidt, H.; Koch, U.; Fotjtik, A.; Baral, S.; Henglein, A.; Kunath, W.; Weiss, Dieman, E. *Chem. Phys. Lett.* **1986**, *124*, 557. (c) Schmidt, H.; Weller, H. *Chem. Phys. Lett.* **1986**, *129*, 615.

(12) (a) Kawabata, K.; Kubo, R. *J. Phys. Soc. Jpn.* **1966**, *21*, 1765. (b) Garniere, I.; Rechststeiner, R.; Smithard, M. A. *Solid State Commun.* **1975**, *16*, 113.

(13) (a) Lushnikov, A.; Simonov, H. *Z. Phys.* **1974**, *270*, 17. (b) Ascarelli, P.; Cini, M. *Solid State Commun.* **1976**, *18*, 385.

(14) (a) Drickamer, H. G. *Acc. Chem. Res.* **1986**, *19*, 329. (b) Drickamer, H. G. *Physica A* **1989**, *156*, 179.

(15) Sandroff, C. J.; King, H. E.; Herschbach, D. R. *J. Phys. Chem.* **1984**, *88*, 5647.

(16) Wilenzick, R.; Russell, D.; Morriss, R.; Marshall, S. *J. Chem. Phys.* **1967**, *47*, 533.

(17) Turkevich, J.; Stevenson, P.; Hillier, J. *Discuss. Faraday Soc.* **1951**, *11*, 55.

(18) Granqvist, C. G.; Buhrman, R. A. *J. Appl. Phys.* **1976**, *47*, 2200.

(19) Okamoto, B. Y. Ph.D. Dissertation, University of Illinois, 1974.

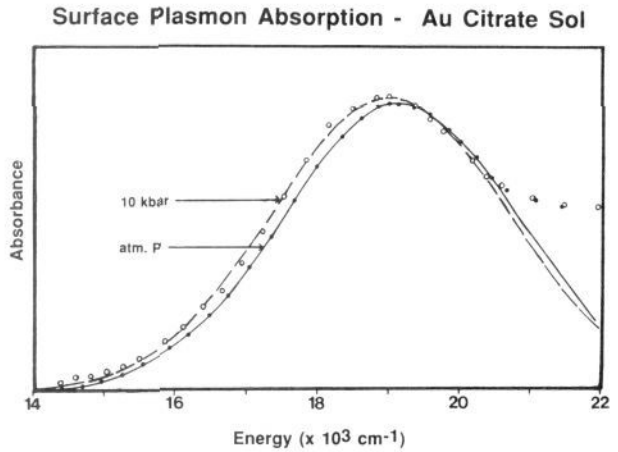

Figure 1. Typical absorption spectra of the surface plasmon resonance of a Au citrate colloid at atmospheric pressure (—) and 10 kbar (---). The overall shift of the peak maximum in this pressure range is approximately 200 cm^{-1}.

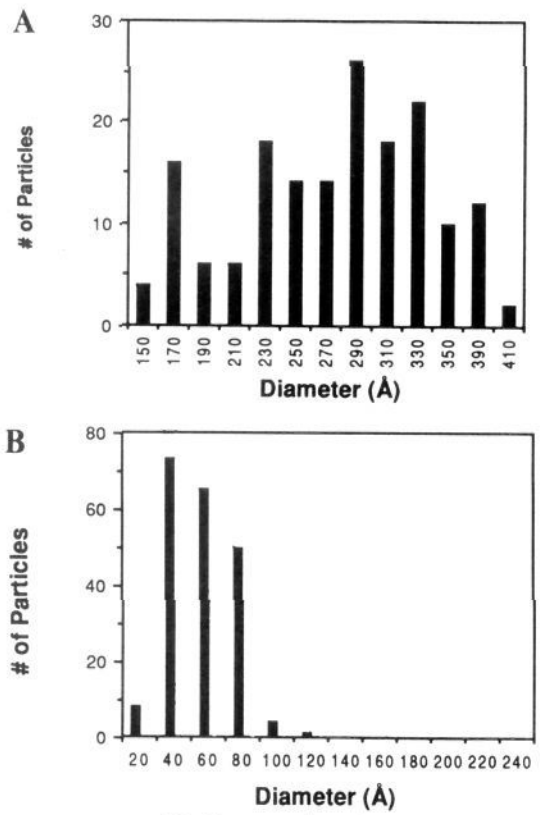

Figure 2. Histograms of freshly prepared Au citrate (A) and Au Faraday (B) sols.

pressure-dependent phenomena were both reversible and reproducible.

Results

Colloidal Gold Particles. For collodial gold particles suspended as a hydrosol, the corresponding surface plasmon absorption peak appears at approximately 19.2×10^3 cm^{-1} (515 nm) at atmospheric pressure (Figure 1). In order to evaluate the effect of pressure on the spectroscopic properties of particles possessing very different average sizes, two methods were utilized: (1) application of the citrate reduction procedure to chloroauric acid solutions generated gold particles with a median particle diameter of 265 Å and a σ value of 1.35; (2) the modified Faraday method generated particles with a median particle diameter of 54 Å and a σ value of 1.56 (Figure 2). Each method generates a range of particle sizes satisfying a log normal distribution. The stark contrast in

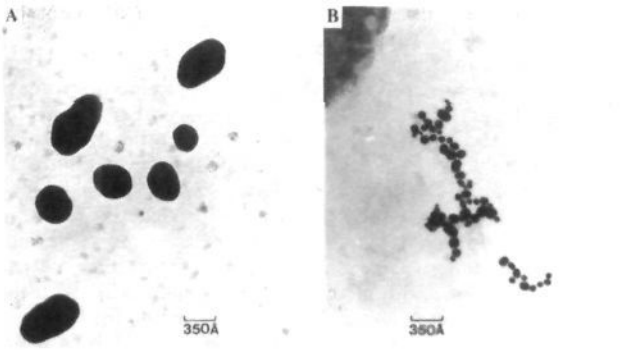

Figure 3. Electron micrographs of freshly prepared Au citrate (A) and Au Faraday (B) sols.

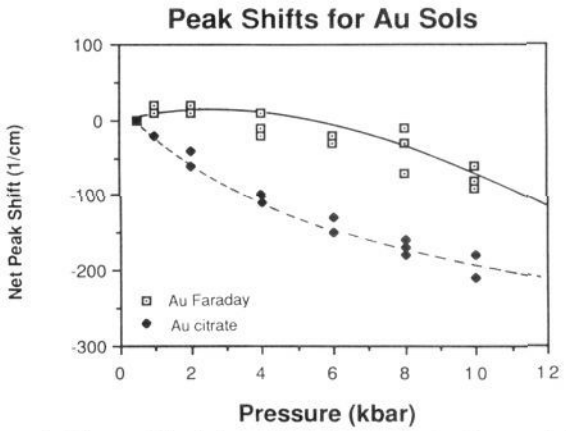

Figure 4. The net shift of the peak maxima of the Au citrate and Au Faraday sols with increasing pressure.

median particle size is most clearly seen by comparing two typical micrographs of these sols (Figure 3).

The effect of pressure on the peak position of the surface plasmon absorption of these gold colloids is illustrated in Figure 4. The surface plasmon absorption peak of the Faraday gold sol (median d = 54 Å) shifts negligibly until ca. 4 kbar, and subsequently shifts slightly red to lower energy overall (−80 cm^{-1}) in 10 kbar. This is in contrast to the citrate sol (mean d = 265 Å) in which the surface plasmon feature shifts continuously red with increasing pressure for a total of approximately −200 cm^{-1} in 10 kbar. Figure 1 shows these differences between atmospheric pressure and 10 kbar for the case of the gold citrate sol. Thus, between the two types of gold particles, there is a marked difference in terms of the shift of the peak position with increasing pressure.

However, we consider the fact that there may be slight differences due to the type of functional group stabilizing each type of metal particle. In the case of the citrate sol, they are carboxylate moieties; for the Faraday sol, they are presumably polyphosphate groups. In order to evaluate the magnitude of such differences on the pressure-induced peak shifts, we allowed the Au Faraday sol (initial diameter of 54 Å) to age at room temperature in the dark for specific periods of time. Aging for 8 weeks resulted in an increase in average particle size to 85 Å and a σ value of 1.40 (Figure 5). Further aging of the sol for an additional 8 weeks resulted in colloids possessing an even larger median particle size (106 Å) with a σ value of 1.65 (Figure 5). Also noteworthy of this 16-week-aged gold Faraday sol is the significant aggregation observed for some particles in the form of rods, chains, and large globular spheres, some of which exhibit sizes up to 500 Å. The corresponding pressure shifts of the surface plasmon peak maxima for each of these two aged colloids are noted in Figure 6. Note the intermediate pressure-induced behavior of the peak shift of these sols: the 8-week-aged gold sample initially shifts red with an overall shift of −130 cm^{-1} in 10 kbar, while the behavior of

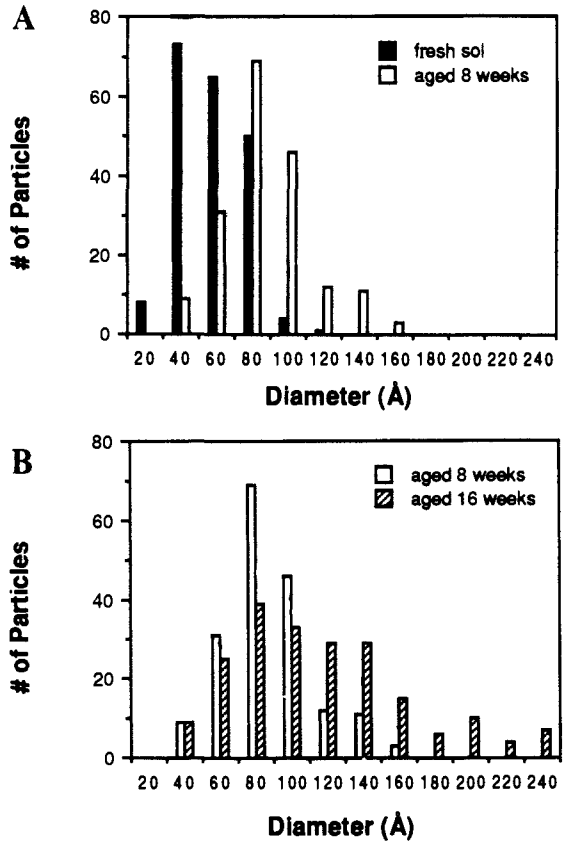

Figure 5. Comparative histograms of freshly prepared and aged Au Faraday sols. Graph A compares the sizes of fresh and 8-week-aged samples, while graph B compares 8-week- with 16-week-aged samples.

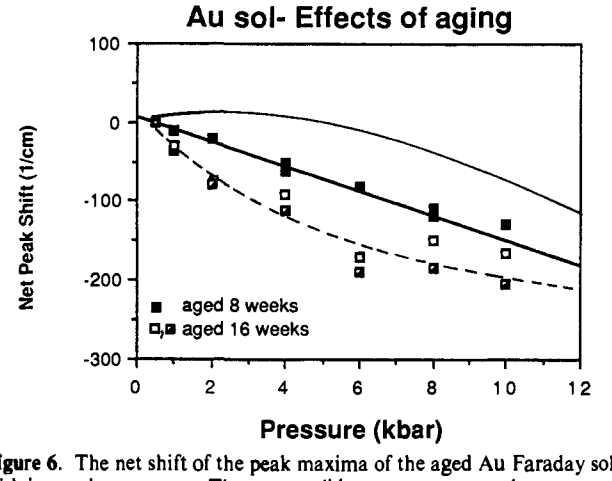

Figure 6. The net shift of the peak maxima of the aged Au Faraday sols with increasing pressure. The upper solid curve represents a least-squares fit to the peak shift of the fresh Au Faraday sol, while the lower dashed curve represents the corresponding fit of the fresh Au citrate sol. For the 16-week-aged sample, □ represents $\omega_0 = 16.5 \times 10^3$ cm^{-1}, while ◪ represents $\omega_0 = 20.0 \times 10^3$ cm^{-1}.

the 16-week-aged sample even more closely resembles that of the citrate sols with a shift of -205 cm^{-1} in 10 kbar. The presence of the large, asymmetric particles in the 16-week-aged sample (in addition to the spherical non-interacting particles) introduces a substantial asymmetry to its surface plasmon absorption, which is consistent with the previous observations of Kreibig for aggregated Au particles.[6b] Thus, we found it necessary to utilize two Gaussian peaks to fit the observed band. The two sets of symbols in Figure 6 for the 16-week sample represent these two separate features; both peaks shift with approximately the same slope with pressure.

It should also be noted that for aged Au Faraday sols, the range of sizes obtained at 8 and 16 weeks conforms to a log normal

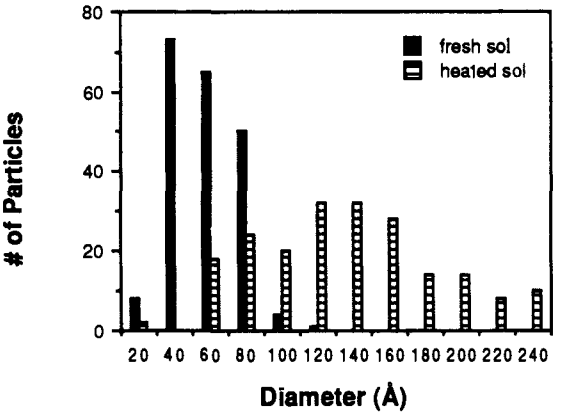

Figure 7. Comparative histograms of a freshly prepared Au Faraday sol with an identical sample heated for 2 h at 75 °C.

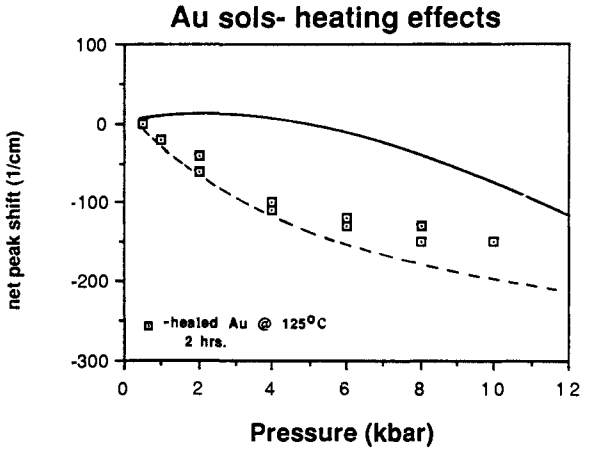

Figure 8. The net peak shift of the peak maximum of a heated Au Faraday sol with increasing pressure. The upper solid curve represents a least-squares fit to the peak shift of the fresh Au Faraday sol, while the lower dashed curve represents the corresponding fit of the fresh Au citrate sol.

distribution and that the retention of log–normal behavior upon aging is consistent with a coalescence growth mechanism noted previously for several types of metal particles.[18]

We next examined a freshly prepared gold Faraday sol which had been heated at 75 °C for 2 h. Examination of this heated sol by high-resolution electron microscopy revealed particles with an average diameter of 128 Å (see Figure 5), negligible contact between particles, and a size distribution that conformed to a log normal distribution ($\sigma = 1.52$). Correspondingly, the pressure behavior of the surface plasmon absorption closely followed that of the citrate sol, especially in the 1–4 kbar region (Figure 7). Thus, regardless of the presence of multiparticle interactions or different specific functional groups at the particle surface, the peak location of these sols of diameter larger than 100 Å is affected by pressure in a strongly analogous fashion.

With regard to changes in full-width at half-maximum (fwhm), all colloidal gold particles examined showed negligible change in this parameter with increasing pressure.

Colloidal Silver Particles. Analogous procedures were utilized to prepare silver colloids, which exhibit a surface plasmon absorption at approximately 20.0×10^3 cm^{-1} (400 nm) (Figure 9). In this case, the citrate procedure generated spherical particles with a median diameter of 230 Å (Figure 10), slightly smaller than those generated for gold by this method. The Faraday method produced silver colloids with a median diameter of 60 Å (Figure 10). For silver, each method also generated a range of particle sizes satisfying a log normal distribution with particles prepared by the citrate method yielding a σ value of 1.21 and those generated by the Faraday method giving a value of 1.80.

The effect of pressure on the peak position of the surface plasmon absorption of these silver colloids is illustrated in Figure

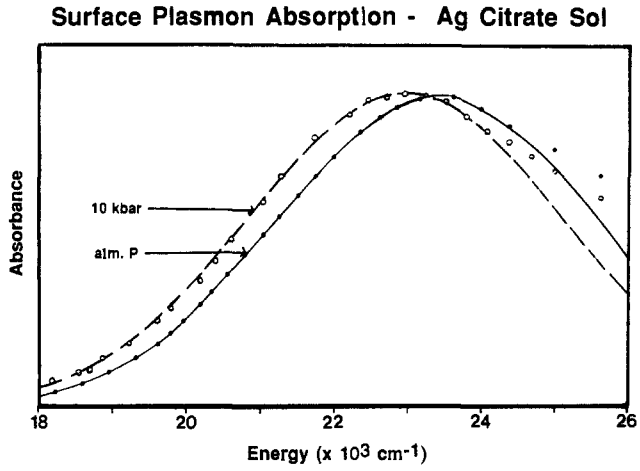

Figure 9. Typical absorption spectra of the surface plasmon resonance of a Ag citrate colloid at atmospheric pressure (–) and 10 kbar (– – –). The overall shift of the peak maximum in this pressure range is approximately 400 cm^{-1}.

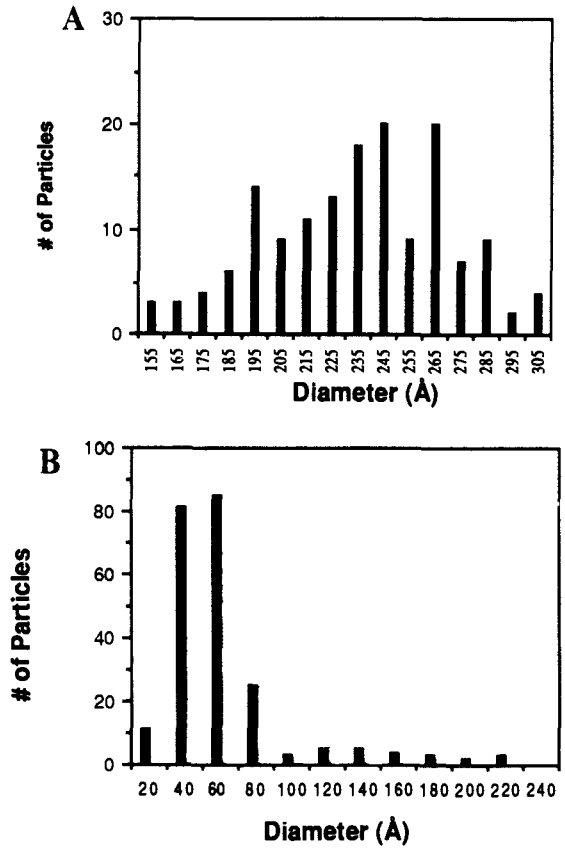

Figure 10. Comparative histograms of freshly prepared Ag citrate (A) and Ag Faraday (B) sols.

11. Note that for silver, the Faraday sol (median d = 60 Å) exhibits a behavior with increasing pressure that mimics the gold Faraday sol in terms of direction but is markedly different in magnitude. While the initial (up to 4 kbar) and overall (10 kbar) shifts of the gold Faraday sol are effectively +20 and −80 cm^{-1}, respectively, those for the analogous silver sol are +200 and −270 cm^{-1}. For the silver citrate particles (median d = 230 Å), there is a continuous red shift of the surface plasmon peak location with a magnitude over two times that of the analogous gold citrate sol (420 cm^{-1} vs 200 cm^{-1} in 10 kbar; see Figure 9).

Once again, aging studies were carried out on the Faraday sol to assess any slight differences due to the type of functional group stabilizing each type of metal particle. Aging the 60 Å silver Faraday sol for 8 weeks resulted in an increase in the median diameter of the particles to 75 Å (Figure 12). Correspondingly,

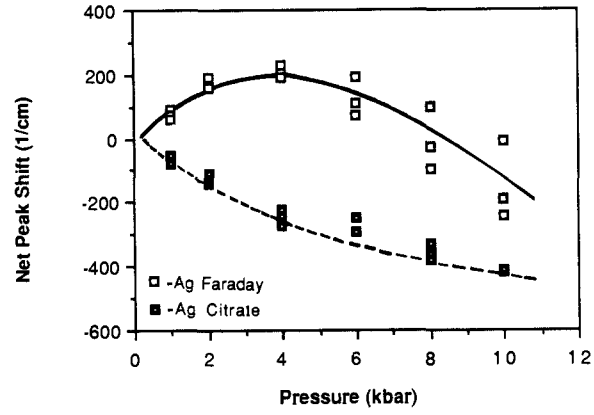

Figure 11. The net shift of the peak maxima of the Ag citrate and Ag Faraday sols with increasing pressure.

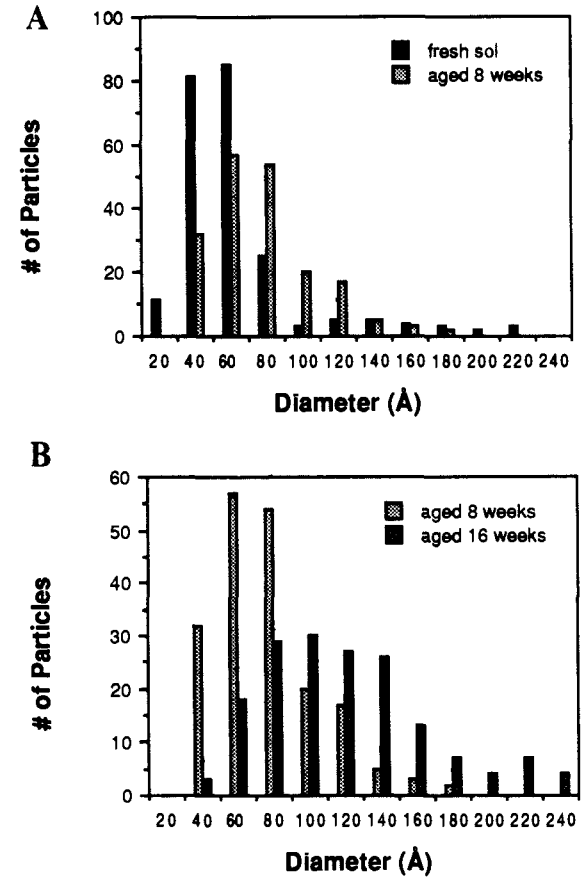

Figure 12. Comparative histograms of freshly prepared and aged Ag Faraday sols. Graph A compares the sizes of fresh and 8-week-aged samples, while graph B compares 8- with 16-week-aged samples.

an intermediate behavior in pressure-induced peak shifts between the two size extremes was observed, as this 75 Å silver sol shifts negligibly up to 4 kbar and then shifted overall 190 cm^{-1} to lower energy in 10 kbar (Figure 13). Allowing this 8-week-aged sample to age another 8 weeks resulted in the formation of particles with a diameter of 111 Å (Figure 12). For this sol, the overall plasmon peak shift also is intermediate between the two extremes, but the differences between this and the 8-week-aged silver sol appear negligible.

In a manner analogous to the aged Au Faraday sols, the range of sizes obtained at 8 and 16 weeks for the aged Ag Faraday sols conforms to a log normal distribution, with σ values of 1.59 and 1.61, respectively. A coalescence growth mechanism of these particles is assumed as well.

As in the case of gold, no significant changes in the fwhm of the surface plasmon resonance absorption of any silver colloids were detected in the pressure range studied.

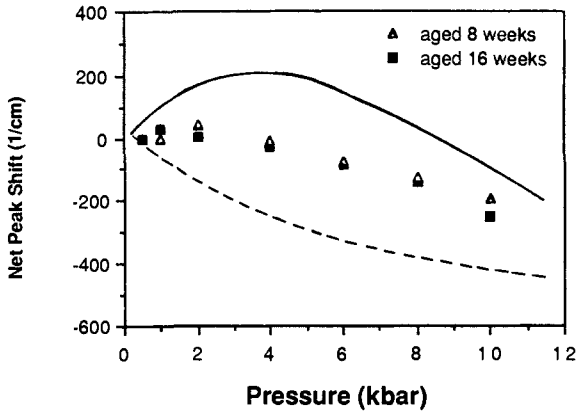

Figure 13. The net shift of the peak maxima of the aged Ag Faraday sols with increasing pressure. The upper solid curve represents a least-squares fit to the peak shift of the fresh Ag Faraday sol, while the lower dashed curve represents the corresponding fit of the fresh Ag citrate sol.

Discussion

For both gold ($\bar{d}$ = 265 Å) and silver ($\bar{d}$ = 230 Å) particles prepared by the citrate procedure, there is a continuous shift to lower energy in the absorption maximum of the surface plasmon resonance with increasing pressure. The magnitude of the shift observed for silver is over twice that for gold (−420 cm^{-1} vs −200 cm^{-1}).

The classical theory for the dielectric response of isolated spherical metal particles is the Mie theory.[9] Its formulation for the surface plasmon peak maximum is usually expressed in terms of the formula shown in eq 1,[9] where ω_p^2 is the bulk plasma oscillation frequency, ϵ^1 is the real part of the dielectric constant of the metal, and ϵ_m is defined as the dielectric constant of the medium:

$$\omega_{sp}^2 = \omega_p^{2/(\epsilon_1+2\epsilon_m)} \quad (1)$$

With regard to changes in the terms of this expression with increasing pressure, the corresponding values of ϵ_1 are 1/20 the magnitude of ϵ_m,[20] and any pressure-induced changes in ω_{sp} would be dominated by this latter term. Specifically for ϵ_m, it is known that the dielectric constant of water increases in a nonlinear fashion by ca. 20% in 10 kbar.[21] Indeed, a plot of ϵ_0/ϵ versus pressure in the 0–10 kbar range shows a curvature closely mimicking that of the pressure-induced peak shifts of the large citrate particles (see Supplementary Material). This increase would predict a red shift of the plasmon peak much larger than observed, although the magnitude of the shift could be dampened by surface effects. However, the most critical flaw of this model is that it alone cannot explain the observation that the differential pressure shift in the surface plasmon peak maximum of silver is a factor of 2 larger for silver than for gold. Thus, this classical theory fails to satisfactorily explain the observed pressure effects.

The surface plasmon may be treated in a quantum mechanical context as deriving from a free-electron gas. In this case the Fermi level energy may be calculated from the expression given in eq 2,[6a,22] where n = number density of the electrons and m = mass of an electron:

$$E_F = h^2(2m)^{-1}(3n/8\pi)^{2/3} \quad (2)$$

Utilizing this equation in conjunction with the known first-order compressibility of gold and silver,[23] we calculate that the Fermi levels of these metals shift 161 and 310 cm^{-1}, respectively, to higher energy in 10 kbar (see Supplementary Material). Thus, the magnitude of these shifts in E_F and relative differences between gold and silver are markedly similar to the observed plasmon peak shifts in this pressure range.

To account for an overall red shift of the surface plasmon resonance, the position of the lowest excited state of the electron gas must, with increasing pressure, remain stationary or shift blue at a rate less than that of the ground state. Extensive precedent exists to support this conclusion. First, it is well-known that π–π^* excitations of organic materials in crystalline or polymeric media shift to lower energy with increasing pressure due to a red shift of the more-polarizable excited-state level relative to the ground state.[24] Second, for the heavier alkali metals (Cs, Rb, K) it is established from resistivity measurements that the excited energy levels of d-band character rate significantly split with increasing pressure.[25] In fact, the width of the d band increases so substantially that above certain pressures (depending on the metal) the bottom of the d band lies energetically *below* the top of the s band. Since gold and silver are far less compressible than the alkali metals[23] (particularly in 10 kbar), the pressure effects on the d bands of Au and Ag may be viewed as an analogous "perturbation". Therefore, shifts of the surface plasmon resonance to lower energy are accounted for within the context to this model.

For the gold and silver particles prepared by the Faraday method, substantial differences were also observed in both the initial (up to 4 kbar) and overall (10 kbar) response to pressure between these sols (median d = 54 Å (Au), 60 Å (Ag)). Since there may be slight differences between these sols and the citrate sols due to the type of functional group stabilizing each type of metal particle, aging experiments were performed on the Faraday colloids of both silver and gold. Examination by electron microscopy at the 8- and 16-weeks-aging periods indicated substantial growth and aggregation of the metal particles, with a response of the surface peak maximum to pressure gradually mimicking that of the citrate metal particles (i.e., a continuous red shift of the plasmon peak maximum with increasing pressure). In the case of gold, isolated spherical particles of median diameter 128 Å can also be generated by prolonged heating of a fresh sol at slightly elevated temperatures (70–75 °C) and the pressure behavior of its surface plasmon resonance most closely resembles that of the citrate sol. Thus, the pressure shifts observed are not dependent on the specific functional group at the particle surface.

While the free-electron gas model provides a satisfactory explanation for the citrate sols, a problem remains in interpreting the blue shifts observed for the Faraday colloids of median diameter 54 Å (Au) and 60 Å (Ag). Clearly the surface-to-volume ratio changes significantly and surface effects (roughness, etc.) take on an even greater importance. Previously, Kreibig has noted that intrinsic size effects in absorption band shape are typically observed for Au particles less than 150 Å in diameter and for Ag particles less than 100 Å.[6b] However, even at atmospheric pressure, changes in the peak location with size of such "quantum-confined" particles are believed to be a superposition of several effects and the debate over which is dominant has yet to be resolved in the literature.[2] We do note, however, that the plasmon peak(s) of the 54 Å Au and 60 Å Ag particles begin to shift red at pressures higher than 4 kbar. Such behavior is typical of an interplay between competing effects, one or more of which begin to dominate at higher pressures.[26]

The final observation to note here is the lack of any detectable changes with increasing pressure in the full-width at half-maximum (fwhm) of the surface plasmon resonance of these hydrosols. The lack of any observed changes is strong evidence that pressure-induced effects do not involve interparticle coupling, as Kreibig has noted previously the sensitivity of line width to multiparticle interactions.[6b] Furthermore, the average calculated distance between freshly prepared particles in solution is on the order of 5–10 μm, and given the compressibility of the surrounding aqueous medium in 10 kbar (ca. 20%), it is difficult to envision significant interparticle coupling with increasing pressure.

(20) Johnson, P. B.; Christy, R. W. *Phys. Rev. B* **1972**, *6*, 4370.
(21) Owen, B. B.; Brinkley, S. R. *Phys. Rev.* **1943**, *64*, 32.
(22) Dekker, A. J. *Solid State Physics*; Prentice-Hall: Englewood Cliffs, NJ, 1957; p 214.
(23) Bridgman, P. W. *The Physics of High Pressure*; G. Bell and Sons: London, 1949; p 161.
(24) Drickamer, H. G. Annu. *Rev. Phys. Chem.* **1982**, *33*, 25.
(25) Stager, R. A.; Drickamer, H. G. *Phys. Rev.* **1963**, *132*, 124. Stager, R. A.; Drickamer, H. G. *Phys. Rev. Lett.* **1964**, *12*, 19. Sternheimer, R. M. *Phys. Rev.* **1950**, *78*, 235.
(26) Mitchell, D. J.; Schuster, G. B.; Drickamer, H. G. *J. Chem. Phys.* **1977**, *67*, 4837.

Conclusions

In this work we have demonstrated, for the first time, the effect of pressure on the peak position of the surface plasmon resonance of colloidal gold and silver particles. For the citrate-derived particles, the observed red shifts and differential behavior of silver vs gold can be interpreted in terms of a free-electron gas model. For the particles prepared by the Faraday method, the pressure-induced peak shifts appear to reflect the much smaller average particle size obtained by this procedure. These results provide evidence that "pressure-tuning" can detect the appearance of a quantum size effect in these metal colloids.

Acknowledgment. This work was supported by grants from the National Science Foundation (DMR 86-12860) and Materials Science Division of the Department of Energy (DE-AC02-76ER01198). The authors thank Peggy Mochel of the Center for Microanalysis of Materials of the University of Illinois (supported under the above DOE contract) for valuable assistance with the electron microscope measurements.

Registry No. Au, 7440-57-5; Ag, 7440-22-4.

Supplementary Material Available: Tables of variances from least-squares fitting of absorption spectra, log-probability plots for each colloid, a plot of normalized pressure-induced changes in the dielectric constant of water, and a graph of the shifts of the Fermi level of gold and silver with increasing pressure (12 pages). Ordering information is given on any current masthead page.

Methane Activation on Unsupported Platinum Clusters

D. J. Trevor,*,† D. M. Cox,* and A. Kaldor

Contribution from Exxon Research and Engineering Company, Annandale, New Jersey 08801.
Received March 14, 1989

Abstract: We report the first observation of size-selective methane activation by unsupported platinum clusters. Platinum dimer through pentamer are the most reactive. The other small clusters, Pt_{6-24}, are less reactive. A factor of 4 drop in reactivity occurs in going from Pt_5 to Pt_6. The dominant products observed are of the form $Pt_nC_{1,2}H_y$. As the clusters increase in size, the number of hydrogens retained also increases. The reactivity tends to decrease with increasing cluster size, in contrast to the trends observed for dihydrogen chemisorption on several transition metals. A mild correlation is found between reactivity and the ability of certain size clusters to form compact structures and the number of ≤3-coordinated surface atoms in close-packed structures found to be most stable from theoretical calculations. These results suggest that, as in organometallic chemistry, coordinative unsaturation is critical for methane activation by naked metal clusters.

Advances in unsupported metal cluster synthesis[1] and characterization methods,[2] combined with the ability to study chemical reactivity,[3] have resulted in a significant increase in the type of systems studied and the amount of information gained. We have demonstrated that ionization potentials, magnetic moments, and chemical reactivity of unsupported metal clusters can be measured and frequently follow nonmonotonic trends from atomic to bulk properties.[4] Such experiments offer a rather direct approach to increasing our understanding of fundamental properties in the transition from molecular to metallic behavior.

Specifically, we have studied the reaction of methane with platinum clusters containing up to 24 atoms. Under our experimental conditions we have found them to activate C-H bonds in methane with certain size clusters being more reactive than others. Provided that our detection is nondestructive, we observe that (1) chemisorbed species are produced at a low extent of reaction whose hydrogen content only slightly varies with cluster size and (2) products produced at high reactant concentrations appear to chemisorb methane with significantly less hydrogen loss. The small clusters undergo facile chemistry not previously observed for either the atom or the bulk. Pt_{2-5} are more reactive than the atom by at least 1 order of magnitude and the bulk by probably several orders of magnitude. Nonmonotonic reactivity is observed to 24 atoms (the largest cluster studied). This is one of the few examples with unsupported transition-metal clusters in which the small clusters are found to be the most reactive species. At low extent of reaction, metal monocarbide peaks are observed for the atom and dimer suggestive of complete dehydrogenation. As the cluster size increases the extend of dehydrogenation decreases, since product peaks consisting of a combination of carbide and $-CH_m$ species are detected. At high extent of reaction, the metal carbide, or $-CH_m$, species appear to continue to chemisorb methane but with minimal dehydrogenation.

Matrix isolation studies of metal atom chemistry have failed to find a ground-state atom,[5] with the possible exception of aluminum,[6,7] that activates methane. However, alkanes including methane are rather easily activated by partially coordinately unsaturated metal centers in many organometallic complexes.[8]

† Present address: AT&T Bell Laboratories, Murray Hill, NJ 07974.

(1) Dietz, T. G.; Duncan, M. A.; Powers, D. E.; Smalley, R. E. *J. Chem. Phys.* **1981**, *74*, 6511. Bondybey, V. E.; English, J. H. *Chem. Phys. Lett.* **1983**, *94*, 443-447. For a review of this field concentrated on spectroscopy see: Morse, M. D. *Chem. Rev.* **1988**, *86*, 1049-1109.

(2) As examples of physical property measurements see the following. (a) Ionization potentials: Rohlfing, E. A.; Cox, D. M.; Kaldor, A.; Johnson, K. H. *J. Chem. Phys.* **1984**, *81*, 3846-3851. (b) Magnetic moments: Cox, D. M.; Trevor, D. J.; Whetten, R. L.; Rohlfing, E. A.; Kaldor, A. *Phys. Rev.* **1985**, *B32*, 7290-7298. (c) Photodissociation: Brucat, P. J.; Zheng, L. S.; Pettiette, C. L.; Yang, S.; Smalley, R. E. *J. Chem. Phys.* **1986**, *84*, 3078-3088.

(3) (a) Trevor, D. J.; Whetten, R. L.; Cox, D. M.; Kaldor, A. *J. Am. Chem. Soc.* **1985**, *107*, 518-519. (b) Whetten, R. L.; Cox, D. M.; Trevor, D. J.; Kaldor, A. *J. Phys. Chem.* **1985**, *89*, 566-569. (c) Geusic, M. E.; Morse, M. D.; Smalley, R. E. *J. Chem. Phys.* **1985**, *82*, 590-591. (c) Morse, M. D.; Geusic, M. E.; Heath, J. R.; Smalley, R. E. *J. Chem. Phys.* **1985**, *83*, 2293-2304. (d) Richtsmeier, S. C.; Parks, E. K.; Liu, K.; Pobo, L. G.; Riley, S. J. *J. Chem. Phys.* **1985**, *82*, 3659-3665. (e) Parks, E. K.; Liu, K.; Richtsmeier, S. C.; Pobo, L. C.; Riley, S. J. *J. Chem. Phys.* **1985**, *83*, 2882-2888, erratum *J. Chem. Phys.* **1985**, *83*, 5353. (f) Cox, D. M.; Trevor, D. J.; Whetten, R. L.; Kaldor, A. *J. Phys. Chem.* **1988**, *92*, 421-429. (g) Zakin, M. R.; Cox, D. M.; Kaldor, A. *J. Chem. Phys.* **1988**, *89*, 1201-1202.

(4) Kaldor, A.; Cox, D. M.; Zakin, M. R. In *Evolution of Size Effects in Chemical Dynamics, Part 2*; Prigogine, I., Rice, S. A., Eds. Advances in Chemical Physics, Vol. 70; Wiley: New York, 1988; p 211.

(5) Billups, W. E.; Konarski, M. M.; Hauge, R. N.; Margrave, J. L. *J. Am. Chem. Soc.* **1980**, *102*, 7393-7394. Perutz, R. N. *Chem. Rev.* **1985**, *85*, 77-96.

(6) Klabunde, K. J.; Tanaka, Y. *J. Am. Chem. Soc.* **1983**, *105*, 3544-3546.

(7) Parnis, J. M.; Ozin, G. A. *J. Am. Chem. Soc.* **1986**, *108*, 1699-1700.

(8) Shilov, A. E. *Activation of Saturated Hydrocarbons by Transition Metal Complexes*; Reidel: Boston, 1984.

0002-7863/90/1512-3742$02.50/0